Spatial position of prepulse induced $J=0 \rightarrow 1$, $3p$-$3s$ lasing in low-Z neonlike ions

Yuelin Li,* Georg Pretzler, and Ernst E. Fill

Max-Planck-Institut für Quantenoptik, Hans-Kopfermann-Strasse 1, D-85748 Garching, Germany†

(Received 13 February 1995)

We report a spatially resolved investigation of lasing on the $3p$ $^1S_0$-$3s$ $^1P_1$ transition in neonlike ions ranging from titanium ($Z=22$) to germanium ($Z=32$). Slab targets were irradiated by the Asterix IV iodine laser at an intensity of about 2.0×10^{13} W/cm^{-2} with a prepulse 5.23 ns before the main pulse. The lasing position was measured as a function of the prepulse energy and the atomic number. It was found that with higher Z, the lasing occurs closer to the target surface and a larger prepulse brings the lasing farther away from the target. A 15% prepulse was found to be favorable for low-Z elements (such as titanium), while a 1.5% prepulse was found to be favorable for elements with Z higher than 26. A simple model taking into account the self-similar expansion of the plasma produced by the prepulse was found to agree qualitatively with the experimental results.

PACS number(s): 42.60.By, 32.30.Rj, 32.70.−n, 52.50.Jm

Since the demonstration of high-gain soft-x-ray lasers in neonlike ions [1,2], the predicted high-gain transition, i.e., the $J=0 \rightarrow 1$, $3p$-$3s$ transition, has shown no or only very low gain until the recent application of the prepulse technique [3–8] and the use of curved targets [9]. The $J=0 \rightarrow 1$ laser dominates the spectra for elements from titanium to germanium when a prepulse is applied [3–8]. It is suggested by simulations [4] that the prepulse plays a key role in modifying the hydrodynamic expansion of the lasing plasma, hence creating a larger, more uniform plasma that reduces losses due to the refraction of the laser beam. Experimentally, it has been verified that refraction and beam divergence of the laser are considerably reduced when a prepulse is used [3–6]. However, direct measurements of the influence of the prepulse on the spatial profile of the lasing region, which could clarify the role of the prepulse, have not yet been performed.

We report in this paper a systematic measurement of the spatial position of the $J=0 \rightarrow 1$ laser in low-Z elements from titanium to germanium, in the presence of a prepulse. The spatial resolution of our diagnostics enabled us to measure the distance of the lasing region from the target surface, which was determined for several materials and two levels of prepulse energy. A simple model, based on a self-similar description of the hydrodynamic motion of the plasma produced by the prepulse (henceforth called *preplasma*), is used to explain the observation, and a good qualitative agreement is obtained. We also measured the dependence of the lasing intensity upon the prepulse energy for varying elements.

The experiment was conducted at the Max-Planck-Institut für Quantenoptik with the Asterix IV iodine laser [10]. Asterix IV delivers up to 800 J of energy at 1.315 μm, with a pulse duration of $\tau=450$ ps [full width at half maximum (FWHM)]. The spurious prepulse of the system was mea-

*Permanent address: Shanghai Institute of Optics and Fine Mechanics, Academia Sinica, P.O. Box 800-211, Shanghai 201800, China.
†FAX: 0049-89-32905-200, Electronic address: yul@ipp-garching.mpg.de

sured below 10^{-6} of the main pulse energy. A line focus was produced by a cylindrical lens array [11]. Each section of the array generates a 30-μm-wide 3.0-cm-long line focus, the overlap of which results in a line focus 150 μm wide and 3.0 cm long. To produce a defined prepulse, a setup similar to those of previous experiments was used [7,8], in which a pair of 17.5×9 cm^2 mirrors with 100% reflectivity at a 60° angle of incidence was inserted into the beam path before and after the final steering mirror. The steering mirror deflects the beam by 60°. The delay between the main pulse and the prepulse was set to $t_d=5.23$ ns. The maximum energy ratio of the prepulse to the main pulse is 15.1%, which is variable by using calibrated filters without changing the energy in the main pulse. Since the prepulse beam intersects only two sections of the lens array, its focus could be narrower than 150 μm, resulting in a higher intensity than that deduced from the energy ratio. The laser illuminated slab targets with lengths of up to 2.5 cm of titanium, iron, nickel, copper, zinc, and germanium ($Z=22, 26, 28, 29, 30, 32$). Typically, a total energy (main pulse plus full prepulse) of 450 J was used, and the shot-to-shot energy variation was ±30 J.

The principal diagnostics was a time-integrated, spatially resolving transmission grating spectrometer coupled to a thinned, backside-illuminated charge-coupled device [12]. It looked axially onto one end of the plasma column, with the spatial resolution in the direction perpendicular to the target surface. The spatial resolution was provided by using a toroidal mirror with a magnification of about 2.6. The acceptance angle of the mirror was limited to 5 mrad, and the spatial resolution was about 50 μm. A 5000-lines/mm freestanding transmission grating with a 50-μm-wide slit dispersed the incident emission perpendicularly to the spatially resolved direction. The wavelength coverage was 3.4–33.2 nm with a spectral resolution of about 0.1 nm. The grating has a supporting structure perpendicular to the grating bars with a period of 4 μm that disperses the incident emission along the spatial direction. The diffraction pattern introduces a spatial structure, which has to be taken into account in the evaluation of the data. The wavelength calibration of the spectrometer was carried out using well-known laser transitions in neonlike germanium at 19.607 ($J=0 \rightarrow 1$), 23.226
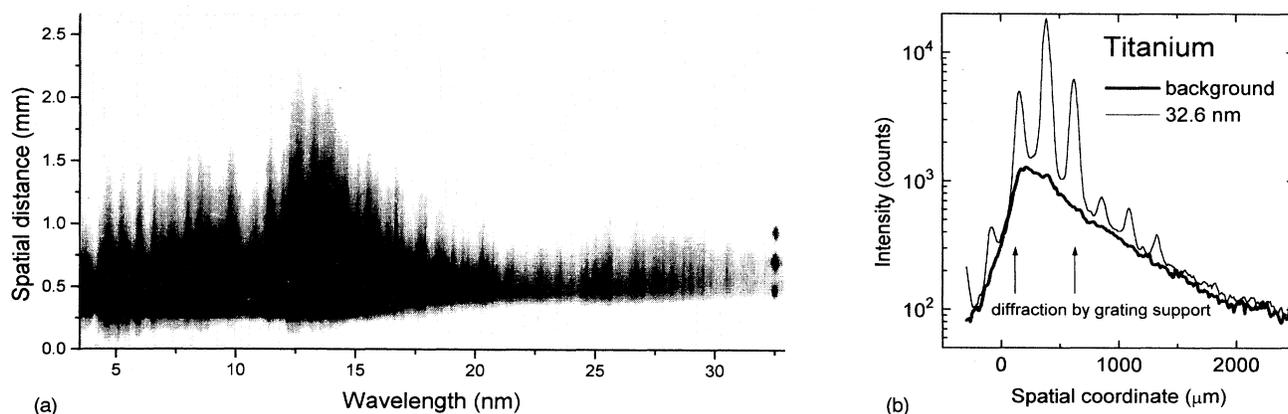
FIG. 1. (a) Spatially resolved spectrum of a 1.2-cm titanium plasma column with a 15% prepulse. The laser at 32.6 nm, accompanied by diffraction due to the 4-μm support structures of the transmission grating, is clearly seen. The scaling of the display is chosen to show the weak emission surrounding the laser spot, so some of the emissions at shorter wavelengths are saturated. (b) Trace along the spatial direction at 32.6 nm and the background close to it from (a). The target surface is at the position 0. The smooth decay at the rear side of the target and the displacement of the background peak emission from the target surface are due to the limited depth of focus of the imaging optics.

($J = 2 \rightarrow 1$), 23.637 ($J = 2 \rightarrow 1$), and 28.649 ($J = 2 \rightarrow 1$) nm. Wavelengths of the $J = 0 \rightarrow 1$ laser in the other elements were found to agree with the previously measured and calculated values [13] within our spectral resolution. They are 32.6, 25.5, 23.1, 22.1, and 21.2 nm in titanium, iron, nickel, copper, and zinc, respectively. Lasing was determined by observing the nonlinear increase of the line intensities with target length.

As an example, a record of the spatially resolved spectrum for a 1.2-cm-long titanium target is given in Fig. 1(a), showing the strong lasing on the $3p\ ^1S_0 - 3s\ ^1P_1$ transition at 32.6 nm. The spatial direction and the dispersion direction are not exactly perpendicular to each other due to a small angle between the grating bars and the target normal. A 15% prepulse was used for this shot with a total energy of 430 J. The bright laser emission, accompanied by the diffraction by the supporting grid, is clearly seen. The central spot gives the spatial position of the lasing, while the two adjacent spots are the $\pm$ first-order diffraction pattern. In Fig. 1(b), the trace along the spatial coordinate of Fig. 1(a) at 32.6 nm and a background close to this lasing line are displayed. Although the diffraction from the supporting structure influences the spatial profile, one can clearly see that the 32.6-nm transition has a maximum displaced from the target surface, with the peak position at about 380 μm from the target. The apparent lasing region is about 60 μm (FWHM) wide, a value that may be slightly influenced by the diffraction due to the grating support. However, this effect should be small since the $\pm$ first orders are separated by a distance considerably exceeding their widths. Therefore, 60 μm is an upper limit of the width of the actual lasing region. As detailed structures in the lasing region cannot be resolved, only the peak position of the laser was measured. The target surface was determined as the crossing point obtained by extrapolating the straight part of the rear slope down to 0 intensity. The error induced in this way was about $\pm$50 μm.

As a first step, the output position of the laser was measured as a function of the target length to observe the influence of refraction. Iron targets of 0.8, 1.2, and 2.4 cm in length were used with a 1.5% prepulse. No substantial difference was observed between 0.8- and 1.2-cm targets, with the laser coming out at 200 and 220 μm from the target surface, respectively. However, for the 2.4-cm target the lasing region was found to be centered at 268 μm, which is explained by refraction of the laser beam. In order to reduce the effect of refraction as much as possible, all the following measurements were done for 1.2-cm targets. A small effect of refraction may still exist for higher-Z targets such as zinc and germanium.

Figure 2 gives the measurement of the lasing peak position as a function of the atomic number under two prepulse conditions. The main pulse energy was kept constant. It is obvious that, as Z increases, the laser moves closer to the target surface. For every element, a larger prepulse carries the lasing region farther from the target surface. The laser intensity in titanium was measured to be as enhanced by a factor of 10 by the 15% prepulse, compared with the 1.5%
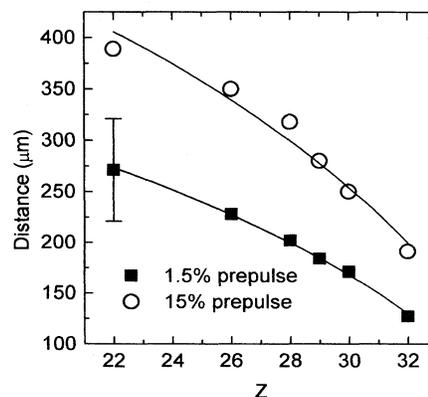
FIG. 2. Distance of the peak lasing position as a function of the atomic number. Prepulses of 1.5% and 15% of the energy in the main pulse were used, while the energy in the main pulse was kept constant. The solid curves are the best fitting by the model described in the text.
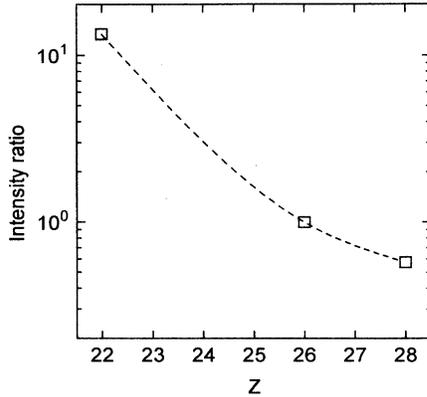
FIG. 3. The intensity ratio of the $J=0\to1$ laser at the 15% prepulse to that at the 1.5% prepulse for titanium, iron, and nickel. The energy in the main pulse was kept constant for the two prepulses.

prepulse. There was no obvious change for iron at the two prepulses, while the laser intensity was decreased by the 15% prepulse in nickel. This is shown in Fig. 3, where the ratios of the laser intensities at the 15% and 1.5% prepulses for titanium, iron, and nickel are given.

These observations can be qualitatively explained by a self-similar model [14] if we assume that the density profile of the lasing plasma is determined by the prepulse and the role of the main pulse is only heating. This implies that, when the main pulse is switched on, the preplasma scale length L_p is considerably larger than its expansion length during the first half of the main pulse. Considering a cylindrical geometry, the mass ablated by the prepulse, and hence the amount of electrons produced, is proportional to $n_c(c_s\tau)^2$, where n_c is the critical density, c_s is the ionic sound speed, and τ is the pulse duration. With self-similar adiabatic expansion, we have a density profile $n_e(r)\sim n_c(\tau/t_d)^2\exp[-(r/L_p)^2]$ for the preplasma when the main pulse is on, with r the distance from the center of the line focus (i.e., the center of symmetry) and $L_p=c_st_d$. t_d is the prepulse–main-pulse delay. If the preplasma is dominated by sodiumlike ions, then $c_s\sim[(Z-10)/A]^{1/2}I_{\text{prepulse}}^{\kappa}$, where A is the ion mass number, and κ is a parameter related to the heating process of the plasma. Analysis gives $\kappa=\frac{1}{3}$ under a steady-state assumption [15]. Using the Z scaling of the optimum electron density for neonlike lasers, i.e., $n_{\text{opt}}=1.5\times10^{15}(Z-9)^{3.75}$ [16], the Z dependence of the lasing is given by

$$r_{\text{peak}}\sim a\left[\frac{Z-10}{2Z}\ln\left(\frac{b}{(Z-9)^{3.75}}\right)\right]^{1/2}, \qquad (1)$$

where the mass number of the ions is approximated by $2Z$. Here b is a dimensionless fitting parameter proportional to $n_c(\tau/t_d)^2$ and depending on atomic physics, hence being *independent* of the prepulse intensity and Z. The other fitting parameter a scales as $\sim I_{\text{prepulse}}^{\kappa}t_d$ and has the dimension of

length. The fits of Eq. (1) to the measured data give excellent agreement, as shown in Fig. 2, with $a=492$ μm, $b=2.03\times10^5$ for the 1.5% prepulse case, and $a=724$ μm, $b=2.12\times10^5$ for the 15% prepulse case, respectively. The fitting parameter b deviates only 5% for the two prepulse conditions. At the ratio of a for the two different prepulses, our fit gives $\kappa=0.17$. We also obtained an initial density at the expanding center from b of $70n_c$, which seems to be independent of the prepulse intensity.

In the above analysis it is implicitly assumed that as long as the temperature T_e reaches the threshold value, the lasing position is not sensitive to it. However, a higher temperature normally results in a higher gain. With the preplasma being assumed to be spatially isothermal and the energy for ionizing the ions being ignored, the temperature of the lasing plasma is inversely proportional to the amount of electrons produced by the prepulse, i.e., $T_e\sim I_{\text{main}}n_c^{-1}c_s^{-2}\tau^{-2}$. Inserting c_s, we have $T_e\sim(1-10/Z)^{-1}I_{\text{main}}I_{\text{prepulse}}^{-2\kappa}\tau^{-2}$. Therefore, the temperature decreases as the prepulse increases. In other words, a bigger prepulse produces more plasma; therefore the energy of the main pulse is shared by more electrons. Furthermore, by taking the Z scaling of $T_e\sim(Z-9)^{3.5}$ [17], we achieve a rough scaling for the optimum prepulse intensity:

$$I_{\text{prepulse}}^{\text{opt}}\sim\left[\frac{I_{\text{main}}}{(1-10/Z)(Z-9)^{3.5}}\right]^{1/2\kappa}.$$

As can be seen, when the main pulse intensity is constant, a smaller prepulse is expected to optimize lasing in a higher-Z target, and vice versa. This explains the tendency of our measurements, as shown in Fig. 3.

In conclusion, we measured the position of the $J=0\to1$ laser in neonlike ions as a function of the prepulse energy and the atomic number. It was found that with higher Z the lasing occurs closer to the target surface and a larger prepulse shifts the lasing farther away from the target. A simple model concerning the self-similar expansion of the preplasma was used to explain the results, and good qualitative agreement was obtained. Regarding the lasing intensity, a 15% prepulse was found to be favorable for low-Z elements (such as titanium), while a 1.5% prepulse was favorable for elements with Z higher than 26, a result that can also be qualitatively explained by our model. Our results verified previous arguments about the role of the prepulse in creating a larger, uniform plasma, which is more suitable for lasing.

[1] D. L. Matthews, P. L. Hagelstain, M. D. Rosen, M. J. Eckart, N. M. Ceglio, A. U. Hazi, H. Medecki, B. J. MacGowan, J. E. Trebes, B. L. Whitten, E. M. Campbell, C. W. Hatcher, A. M. Hawryluk, R. L. Kauffman, L. D. Pleasance, G. Rambach, J. H. Scofield, G. Stone, and T. A. Weaver, Phys. Rev. Lett. **54**, 110 (1985).

[2] T. N. Lee, E. A. Mclean, and R. C. Elton, Phys. Rev. Lett. **59**, 1185 (1987).

[3] T. Boehly, M. Russotto, R. S. Craxton, R. Epstein, B. Yaakobi, L. B. DaSilva, J. Nilsen, E. A. Chandler, D. J. Fields, B. J. MacGowan, D. L. Matthews, J. H. Scofield, and G. Shimkaveg, Phys. Rev. A **42**, 6962 (1990).

[4] J. Nilsen, B. J. MacGowan, L. B. Da Silva, and J. C. Moreno, Phys. Rev. A **48**, 4682 (1993).

[5] J. Nilsen, J. C. Moreno, B. J. MacGowan, and J. A. Koch, Appl. Phys. B **57**, 309 (1993).

[6] J. Nilsen and J. C. Moreno, Opt. Lett. **19**, 1139 (1994).

[7] E. E. Fill, Y. Li, D. Schloegl, J. Steingruber, and J. Nilsen, Opt. Lett. **20**, 374 (1995).

[8] Observation of lasing on the two $J = 0 \rightarrow 1$, $3p$-$3s$ transitions at 26.1 and 30.4 nm in neonlike vanadium, Y. Li, G. Pretzler, and E. E. Fill, Opt. Lett. (to be published).

[9] R. Kodama, D. Neely, Y. Kato, H. Daido, K. Murai, G. Yuan, A. MacPhee, and C. L. S. Lewis, Phys. Rev. Lett. **73**, 3215 (1994); H. Daido, R. Kodama, K. Murai, G. Yuan, M. Takagi, Y. Kato, I. W. Choi, and C. H. Nam, Opt. Lett. **20**, 61 (1995).

[10] H. Baumhacker, G. Brederlow, E. Fill, Ch. Schroedter, R. Volk, S. Witkowski, and K. J. Witte, Laser Part. Beams **11**, 353 (1993).

[11] W. Chen *et al.*, in *1990 Conference on Laser and Electro-Optics*, Technical Digest Series Vol. 7 (Optical Society of America, Washington DC, 1990), pp. 282 and 283.

[12] Y. Li, G. D. Tsakiris, and R. Sigel, Rev. Sci. Instrum. **66**, 80 (1995).

[13] J. Nilsen and J. H. Scofield, Phys. Scr. **49**, 588 (1994).

[14] J. Pert, J. Fluid Mech. **100**, 257 (1980).

[15] See, for example, C. E. Max, in *Laser-Plasma Interaction*, edited by R. Balian and J-C. Adam (North-Holland, Amsterdam, 1982), p. 306.

[16] R. C. Elton, *X-Ray Lasers* (Academic, San Diego, 1990), p. 107.

[17] M. D. Rosen, R. A. London, and P. L. Hagelstein, Phys. Fluids **31**, 666 (1988).